Oil & Gas Science and Technology - Rev. IFP Energies nouvelles **74**, 23 (2019)

https://doi.org/10.2516/ogst/2018102

Available online at:
ogst.ifpenergiesnouvelles.fr

REGULAR ARTICLE OPEN ACCESS

Experimental investigation of two-phase relative permeability of gas and water for tight gas carbonate under different test conditions

Teng Wan[1,2], Shenglai Yang[1,2,*], Lu Wang[1,2], and Liting Sun[1,2]

[1] State Key Laboratory of Petroleum Resources and Prospecting, China University of Petroleum, Beijing, China
[2] Key Laboratory of the Ministry of Education of Petroleum Engineering, China University of Petroleum, Beijing, China

Received: 24 August 2018 / Accepted: 13 December 2018

Abstract. Currently, tight carbonate gas reservoir has received little attention due to few discoveries of them. In this study, gas–water two-phase relative permeability was measured under two different conditions: High Temperature High Pore Pressure (HTHPP – 80 °C, 38 MPa), as well as Ambient Condition (AC), using whole core samples of tight gas carbonate. Relative permeability curves obtained at HTHPP showed two contrary curve profiles of gas relative permeability, corresponding to the distinctive micro-pore structure acquired from CT-Scanning. Then, based on Klinkenberg theory and a newly developed slip factor model for tight sandstone, slippage effect under AC is calibrated and the overestimation of gas relative permeability prove up to 41.72%–52.34% in an assumed heterogeneity. In addition, relative permeability curves obtained at HTHPP switch to higher gas saturation compared to that under AC with the rock wettability change from water-wet to less water-wet. And the wettability alteration is believed to be caused by charge change on mineral surface.

1 Introduction

Tight gas plays an important role in world unconventional gas reserves including Shale gas, Coalbed Methane (CBM), Gas hydrates, etc. (Islam, 2015) and it is defined as gases trapped in very low permeability formations, primarily sandstones and some carbonates (Satter and Iqbal, 2016). Until now, tight gas sandstones have gone through a lot of investigations while there are few studies focusing on tight carbonate gas reservoirs due to few discoveries of them. The only reported tight carbonate gas reservoirs are the Trenton Ordovician field in the northern part of Appalachia, the Upper Cretaceous Austen Cretaceous and lower Cretaceous James Lime in eastern Texas (Cumella *et al.*, 2014), as well as in Sichuan and Ordos basin in China (Wei *et al.*, 2017). However, there are few publications about them.

During the process of gas field development, reservoir simulation is a major method to make a design and decision. And relative permeability, which characterizes the multiphase flow in porous media, is one of the most important parameters for the simulation (Bignonnet *et al.*, 2016). However, the available data associated with relative permeability of tight gas carbonate is few. Recorded experimental research of relative permeability is usually conducted at Ambient Condition (AC) or low pore pressure in laboratory due to its simplicity and rapidity, whereas the result is of great difference with that obtained under reservoir condition. Therefore, it may result in huge mistakes when these curves obtained at AC are input to reservoir simulators. Distinctions of relative permeability under these two conditions can originate from many aspects, such as: wettability alteration and slippage effect.

Wettability affects relative permeability because it controls the fluid location and distribution in the pore space. Anderson (1987) made a comprehensive review about the effect of wettability on relative permeability. The conclusion is that at any given saturation, water phase relative permeability increases, while the oil phase relative permeability decreases when the wettability shift from water-wet to oil-wet. Reservoir wettability is a demonstration of the thermodynamic equilibrium between reservoir fluids and rock surface. And the wettability alteration is actually the ionic interaction in different environmental conditions. Mechanisms of carbonate wettability alteration by low salinity flooding have received much attention in the past few years, and they can be categorized into the following two aspects:

1. *Mineral dissolution.* Hiorth *et al.* (2010) proposed mineral dissolution by history matching the spontaneous imbibition experiments in chalk. The opinion is that organic materials in rock surface could desorb

* Corresponding author: yangsl05@163.com

into the brine when the rock mineral dissolves, and hence the wettability is changed. Using Nuclear Magnetic Resonance (NMR), Yousef *et al.* (2011) supported this idea by presenting an enhancement of micro and macro pore connectivity after low salinity flooding. Austad *et al.* (2011), Esmaeilzadeh *et al.*, (2018) pointed out that the increase of sulfate concentration and ion exchange on the surface were mainly caused by anhydrite dissolution. Nasralla *et al.* (2015) simulated the calcite–brine interaction in their PHREEQC-coupled reservoir simulator, and believe that mineral dissolution is not the main mechanism in their experiment. Mahani *et al.* (2015) confirmed that precipitation only happens at increased pH or alkalinity from different aspects: lab test and PHREEQC simulation.

2. *Charge change on mineral surface.* Many studies have showed an agreement on that the charge at the carbonate surface strongly depends on the salinity, components and pH of the brine as well as the mineral composition and temperature. Alotaibi *et al.* (2011) measured the zeta potential for limestone and dolomite rocks with different formation brines. This study shows that low-salinity water created more negative charges on limestone and dolomite particles. Individual divalent cations decreased the zeta potential of limestone particles in sodium chloride solutions, while sulfate ions showed a negligible effect. Mahani *et al.* (2015) measured the zeta potential of limestone and dolomite in several different brine compositions. The study revealed a good consistence between the charge change on rock/brine surface and wettability change. Zeta potential change versus pH for dolomite-NaCl (2540 mg/L) shows an opposite trend to other brine compositions. A logarithmic dependence of zeta-potential on Ca^{2+} and Mg^{2+} concentration changes was suggested by Alroudhan *et al.* (2016) using the streaming potential. However, all the mechanism investigations for carbonate wettability alteration are focused on the carbonate oil reservoir, whose fluid compositions and interfacial properties are quite different from the gas reservoir.

Klinkenberg effect is an inevitable phenomenon in gas–liquid two-phase flow under low pressure especially for tight reservoirs. And it can cause significant overestimation on gas relative permeability, while this effect could be eliminated at high pore pressure (Li *et al.*, 2009; Sander *et al.*, 2017). However, a few studies have focused on two-phase slippage effect and most of them are qualitative. The effect of gas slippage on gas-liquid relative permeability was firstly studied by Estes and Fulton (1956), Fulton (1951) and Rose (1948). A couple of investigators studied the influential degree of slippage effect caused by different factors, such as: net confining pressure (Sampath and Keighin, 1982), temperature and water saturation (Li and Horne, 2001; Rushing *et al.*, 2003). In addition, Liu *et al.* (2011) and Rushing *et al.* (2003) obtained an empirical correlation of slip factor as a function of water saturation and Klinkenberg permeability. Recently, Li *et al.* (2018) proposed an effective slip factor model based on idealized capillary bundle model, and a heterogeneity coefficient was introduced to characterize the heterogeneity of porous media:

$$b_{\text{eff}} = b_0(1 - S_{\text{w}})^{-m} \qquad 0.5 < m < 2.0, \tag{1}$$

where b_{eff} is the effective slip factor under certain water saturation, b_0 is the slip factor of single gas phase, m is the heterogeneity coefficient ranging from 0.5 for idealized homogeneous media to 2.0 for heterogeneous media, S_{w} is the water saturation.

In this work, gas–water two-phase relative permeability of tight gas carbonate was measured under two different conditions (HTHPP [High Temperature High Pore Pressure], AC) by unsteady state method on whole core samples. Features of relative permeability curves were characterized and analyzed combined with the micro-pore network acquired from CT-Scanning. Thereafter, relative permeability obtained at two different conditions was compared from the perspective of wettability alteration after slippage calibration. It is promising that the results will be beneficial for the future development of tight carbonate gas reservoir.

2 Experimental section

2.1 Experimental samples and fluids

The whole core samples were chosen from the dolomite reservoir at Sichuan Basin, China, in order to minimize the deviation of produced water and better characterize the heterogeneity by this large dimension. Five representative core samples were selected to conduct relative permeability test at HTHPP, and three of them were also tested at AC. Diameter of these rock samples is in the range of 65–70 mm, and the length of them is more than 100 mm which could be supposed to efficiently weaken the capillary end effect. Their physical properties are listed in Table 1.

For completely saturating the pore space, samples were firstly dried for 10 h, and subsequently were vacuumed more than 24 h. Then the same vacuumed brine was injected into the core samples for at least 5 pore volume. Finally, the core samples were taken out to weigh the saturated water and the porosity was calculated accordingly.

A light brine (made of 0.3% wt sodium chloride solution) was used as displaced phase, while nitrogen with a purity of 99.99% was used as displacing phase. A PVT simulator, CMG WinProp (CMG, 2003), was used to obtain gas and brine viscosity and compressibility factor. The evaporation of water could be greatly prevented under HTHPP (80 °C, 38 MPa) (Counsil, 1979), according to Raoult's and Dalton's laws. The physical properties of fluids are summed up in Table 2.

2.2 Experimental differential pressure

A dimensionless group called capillary number, Nc, is always used to characterize the balance of viscos to capillary forces. It is generally defined as follows (Moore and Slobod, 1956; Pini and Benson, 2013):

Table 1. Characteristic data related to physical properties and relative permeability.

Sample	Porosity (%)	Klinkenberg permeability (mD)	Differential pressure (MPa)	Critical gas saturation	Irreducible water saturation	Cross point gas saturation
b	6.74	0.0415	2.31	0.09	0.45	0.33
c	2.15	0.0005	7.12	0.17	0.49	0.28
d	0.83	0.0818	1.45	0.22	0.58	0.34
e	5.41	0.2610	0.28	0.06	0.22	0.45
f	3.84	0.0130	3.96	0.15	0.48	0.32

$$\mathrm{Nc} = \frac{v\mu_{\mathrm{d}}}{\sigma}, \tag{2}$$

where v is the flow velocity (m/s), μ_{d} is the viscosity (cp), σ is the interfacial intension (mN/m).

In order to comply with actual reservoir condition, a relatively low but appropriate flow rate was chosen to conduct this experiment according to equation (2), then the corresponding Differential Pressure (DP) is determined according to Darcy's law.

Table 2. Physical properties of fluids used in the experiment.

Condition	Fluid	Viscosity (cp)	Compressibility factor	Interfacial tension (mN/m)
HTHPP	Nitrogen	0.028	1.222	50.12
	Brine	0.392	0.246	
AC	Nitrogen	0.019	1.000	71.25
	Brine	0.934	–	

2.3 Experimental set up and procedure

The multiple function displacement system was connected mainly by injection pump, gas/liquid storage cylinders, core holder and outlet system comprised by gas/liquid separation, high-accuracy gas mass flow meter, etc., as illustrated in Figure 1. This newly developed experimental apparatus was made of titanium alloy so as to bear a high stress up to 180 MPa and a high temperature up to 200 °C. The effluent fluid was collected during the flooding process and the average calcium concentration was obtained by titration accordingly. Rock samples were soaked in the brine for 2 days before contact angle measurement in order to model the wettability alteration in core-flooding process. Subsequently, the contact angle of nitrogen-brine-rock and pH value of brine were measured.

All experiments were conducted under constant pressure mode and equal effective stress. For the tests under HTHPP, the first step is to elevate the temperature and pressure. The temperature was elevated to the set value (80 °C) and kept constant at least for 24 h to make sure the whole system can reach the required temperature. Then, the pressure was started to establish to avoid the pressure fluctuation when establishing the temperature and pressure simultaneously. Also, the pressure was applied step by step to prevent the stress sensitivity of the core samples.

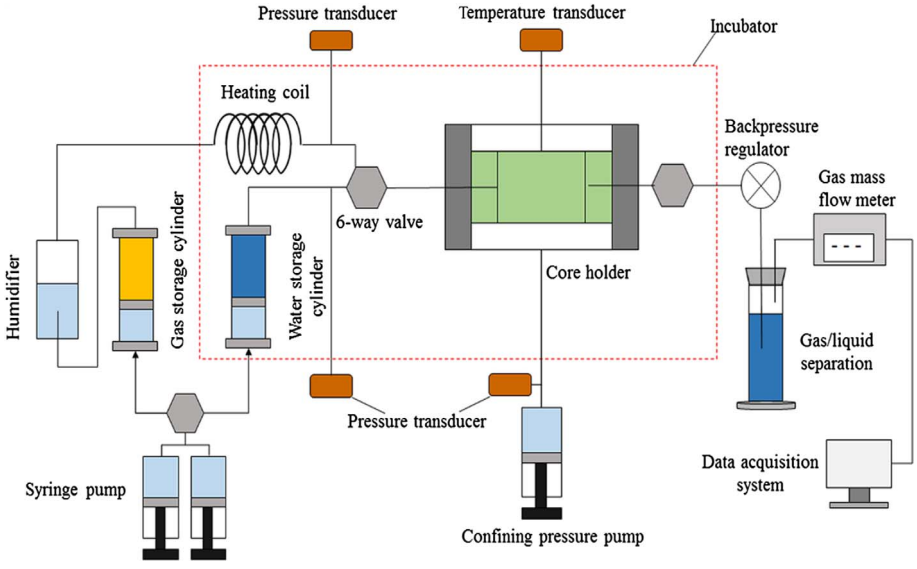

Fig. 1. Experimental system for relative permeability measurement.

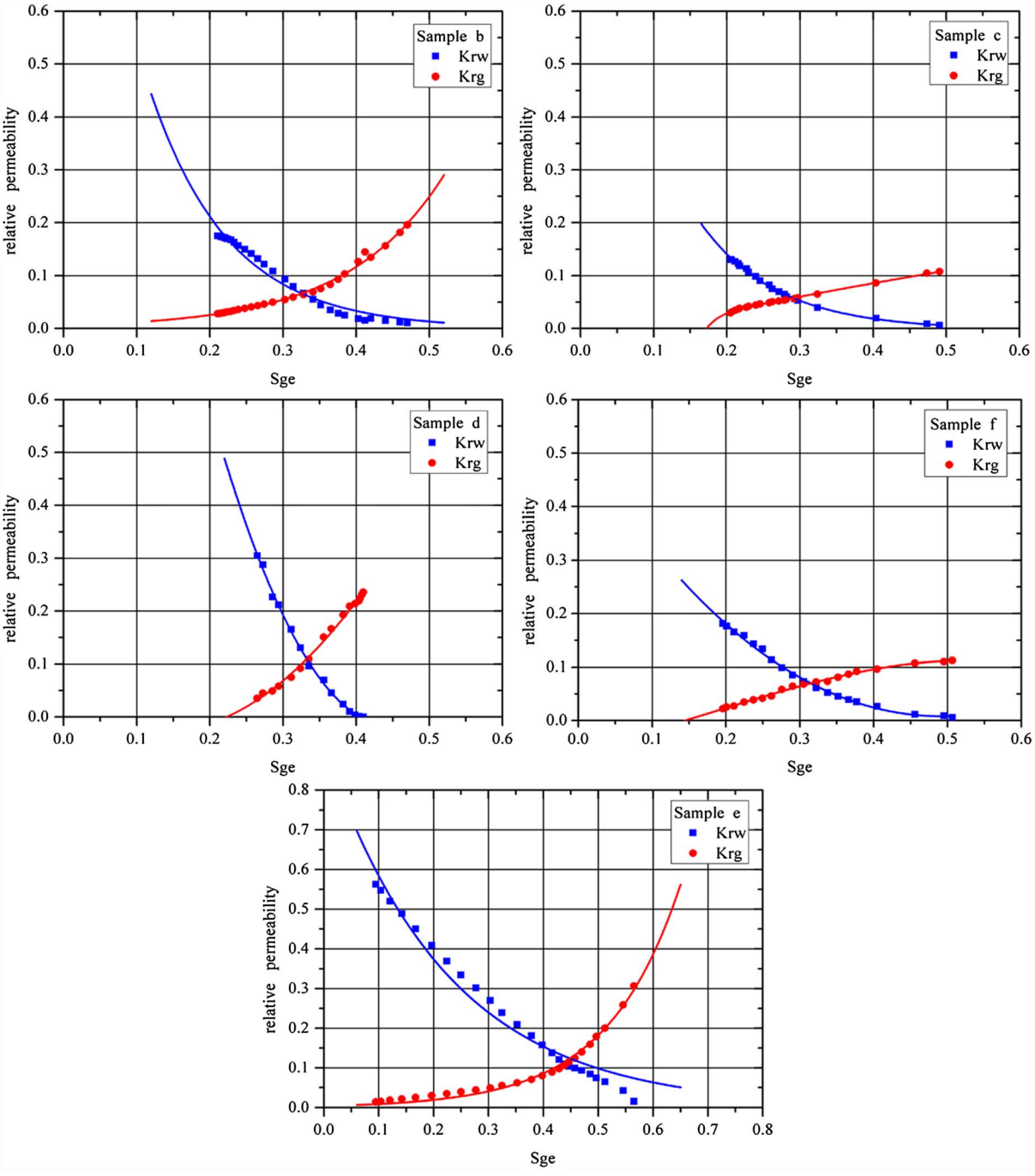

Fig. 2. Examples of relative permeability curves under HTHPP for tight gas carbonate.

Experimental procedures under AC (without backpressure, 25 °C) are the same as that at HTHPP just with the elevation of temperature and pressure removed.

2.4 Calibration of experimental data

The cumulative volume of gas and water collected at Ambient Condition (AC) were corrected to the condition of the core inner according to the state equation. Then, the relative permeability was calculated by JBN method (Johnson *et al.*, 1958).

3 Results and discussion

3.1 Characterization of relative permeability under HTHPP

Five representative relative permeability curves were obtained as presented in Figure 2 and the characteristic data of relative permeability are listed in Table 1.

The most obvious distinction in these curves is that core d displays a steep curve with narrow two-phase seepage area and high residual water saturation. This sample possesses

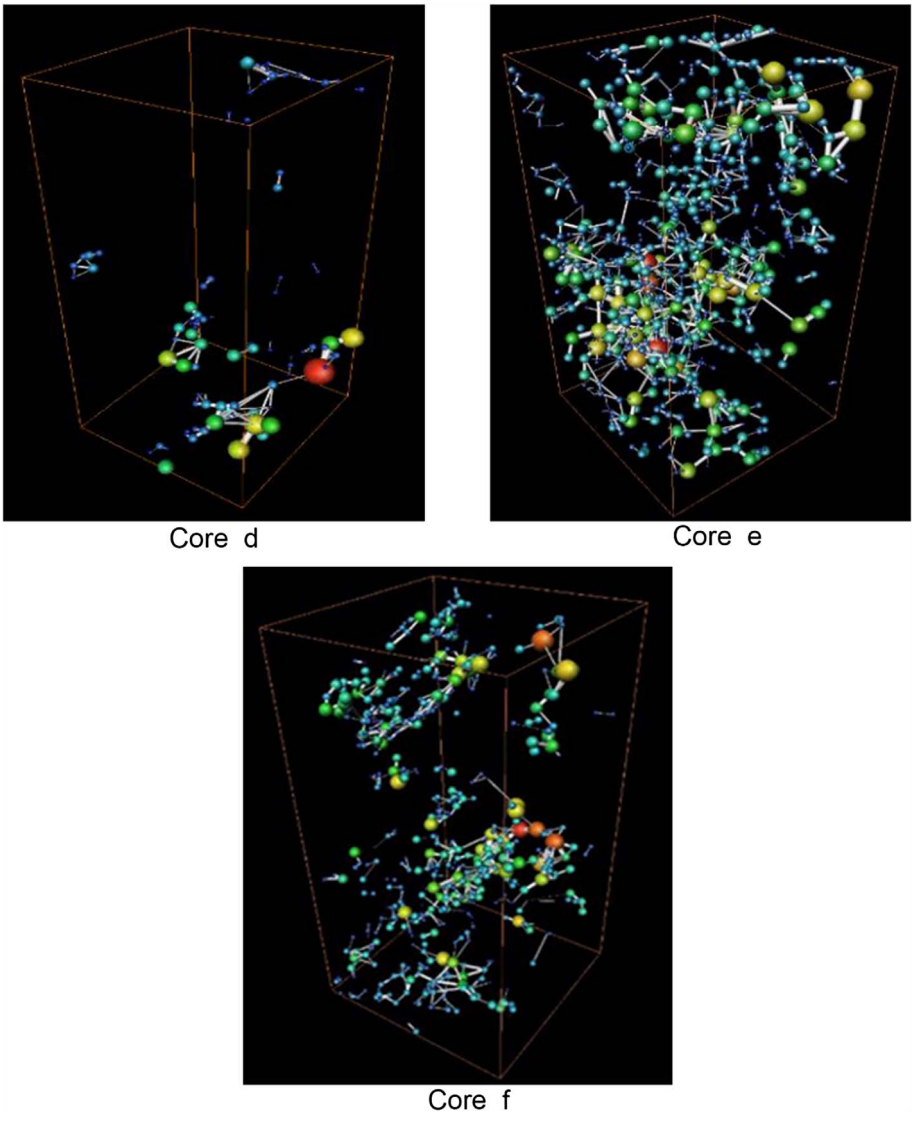

Fig. 3. Three-dimensional micro-pore network obtained from CT-Scanning (from the top to bottom, from left to right are for sample d, e and f respectively).

the highest permeability but the lowest porosity among these samples, which is caused by the existence of several visual fractures as well as extremely few developments of micro-pores as shown in Figure 3. This kind of pore structure suggests fracture is the main pore space for fluid storage and flow, and thus makes it easy to arise fluid channeling and bypassing, which is mainly responsible for this "X" type curve.

As for the other four core samples, notably cores c and f have analogously convex curve of gas phase while cores b and e have a similarly concave curve. The convex curve shape usually indicates the insufficient flow occurring in the micro pore space due to the existence of some extremely small pore throat. In other words, a bad pore space connectivity exists in cores c and f, as shown in Figure 3. From the pore network graph of core f, we observe that although some pore space in both ends of this sample is developed, it is discontinuous in the middle, reflecting the strong heterogeneity in tight gas carbonate. On the contrary, the concave shape implies that the water is easier displaced when there is a better pore space connectivity as shown in the pore network graph of core e in Figure 3, although the pore space may exist interference between two phases. Generally, the concave degree of curve could reflect the strength of multiphase interference during displacing, the more concave, the severer the disturbance (Bachu and Bennion, 2008). However, this interference will not exist in fractured samples as can be seen from core d in Figure 2.

All these measured core samples are water-wet as the cross-point gas saturation is less than 0.5. Without considering the fractured samples, the characteristic data of the other four samples generally display an interrelation with absolute permeability: the higher the absolute permeability, the lower the critical gas saturation and irreducible water saturation, as listed in Table 1.

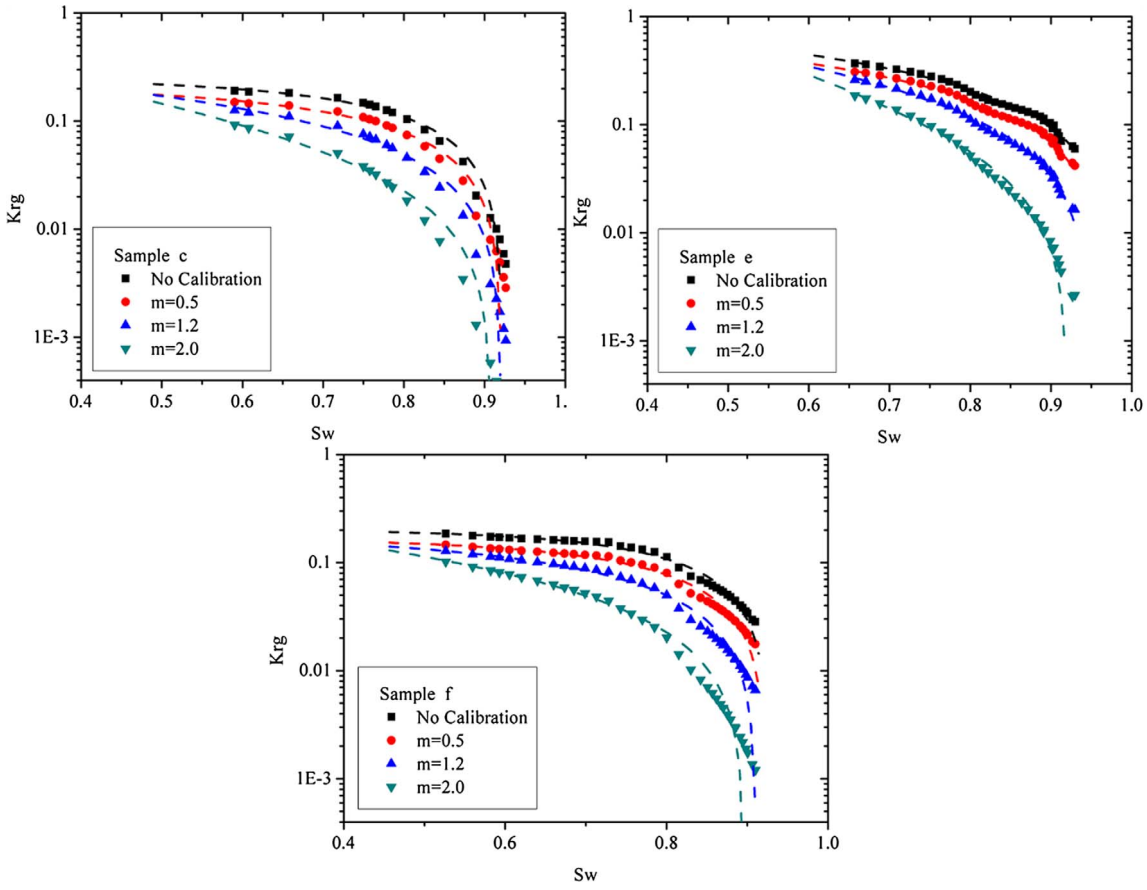

Fig. 4. Impact of Klinkenberg effect on gas relative permeability.

3.2 Calibration of Klinkenberg effect under AC

Combing equation (1) with Klinkenberg theory, the following slippage calibration model under certain water saturation can be obtained:

$$K_{rs} = \frac{K_{rg}}{\left(1 + \frac{b_0(1-S_w)^{-m}}{P}\right)}, \quad (3)$$

where K_{rg} is the apparent gas relative permeability under certain water saturation, K_{rs} is the corrected gas relative permeability accordingly.

Equation (3) was used to correct apparent gas relative permeability measured at AC. The advantage of this calibration model is that it was established based on the classical theoretical capillary model, which could reasonably address this problem from the essential perspective. Due to the difficulty to characterize the heterogeneity (value of m) precisely, we selected three different heterogeneous efficiencies ($m = 0.5$; 1.2; 2.0, from relative homogeneity to a strong heterogeneity) to make this calibration, thus the calibrated results locate in a certain scope as depicted in Figure 4.

Figure 4 shows the calibrated relative permeability of three core samples. It is obvious that gas relative permeability could be significantly overestimated without Klinkenberg correction and there exists a more serious slippage effect with a stronger heterogeneity (larger value of m). Because of the difficulty to quantify heterogeneity, three different corrected curves under corresponding heterogeneity coefficients are displayed. In the following section, the calibrated curve with an intermediate heterogeneity (the blue dash line, $m = 1.2$) is used for analysis.

The error values in gas relative permeability caused by slippage effect for cores c, f and e under 0.65 water saturation are 52.34%, 44.84% and 41.72% respectively, showing the tendency of an increasing error value with a tighter sample. And it is also consistent with classical Klinkenberg theory. In comparison, these error values are much higher than those obtained by Li *et al.* (2018) whose maximum error value is approximate 20%. This can be attributed to the difference in base permeability which is exactly the apparent permeability of single phase in the work of Li *et al.* (2018). It can be corrected in an infinite pressure but will give rise to extreme underestimation of apparent gas relative permeability under AC. In addition, the core samples used in this study are extremely tight promoting the slippage effect.

3.3 Comparison of relative permeability between different conditions

Calibrated relative permeability curves with an average heterogeneity coefficient ($m = 1.2$) are displayed in

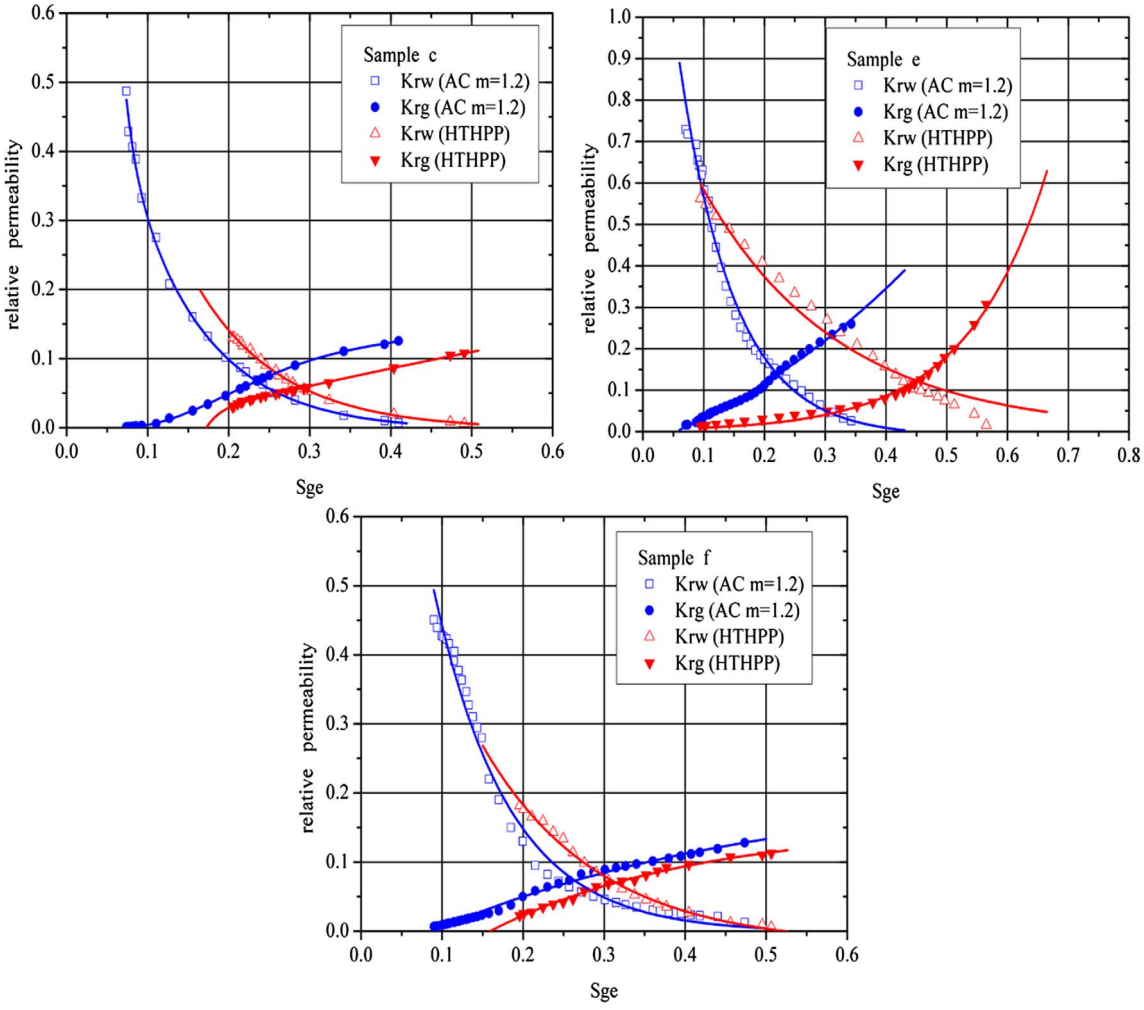

Fig. 5. Comparison of relative permeability under HTHPP and AC.

Table 3. Parameter comparison between different conditions.

Sample	Condition	Differential pressure (MPa)	Capillary number	Contact angle (°)	pH	Calcium concentration (mg/L)	Water production before breakthrough/cumulative water production (%)
c	AC	8.36	9.25E-09	36	7	1	12.67
	HTHPP	7.12	2.68E-08	45	5.5	5	61.87
f	AC	3.5	1.41E-08	40	7	1	17.58
	HTHPP	2.3	3.13E-08	49	5.5	6	76.68
e	AC	0.45	1.46E-08	39	7	2	23.28
	HTHPP	0.28	2.42E-08	65	5.0	8	64.89

Figure 5, associated with corresponding curves obtained at HTHPP. According to previously published studies (Delshad *et al.*, 1986; Reynolds and Krevor, 2015), the capillary number difference has marginal effect on relative permeability around the order of 10^{-8}. As shown in Table 3, relative permeability difference is mainly caused by wettability alteration which is indicated by the contact angle change.

As shown in Figure 5, there are differences in the relative permeability curves under these two conditions. The first is that the relative permeability curve shifts to a higher gas saturation when the test condition changed from AC to HTHPP. At a given saturation, the gas relative permeability decreases, while the water relative permeability increases when the rock wettability change from strong water-wet to less water-wet. This phenomenon is in a good

agreement with that presented by McCaffery (1973) who measured the relative permeability of nitrogen/liquid under different wettability. However, the mechanism of wettability alteration is usually complex and difficult to explain precisely. The potential mechanisms of wettability alteration in this study are examined and analyzed in two aspects as below:

1. *Mineral dissolution.* As shown in Table 3, mineral dissolution surely happens when increases the temperature and pressure, but the solubility is small versus to brine salinity and thus have little effect to enhance brine pH. And it is known in gas reservoir, there barely no desorption of organic materials with dolomite dissolution in the rock surface. Besides, precipitation is also negligible due to the low salinity and neutral and weakly acidic pH of the brine. Therefore, the wettability alteration process caused by mineral dissolution is unable to occur in this study.
2. *Surface charge change.* As the increase of temperature and pressure, the ionization degree of sodium chloride solution increases and hence decreases the pH of brine. Zeta potential of dolomite-NaCl is inversely proportional to the value of pH, which is attested by Mahani *et al.* (2015). As a result, it is to believe that the increase of zeta potential at dolomite surface leads to the increase of contact angle from AC to HTHPP condition. This result is opposite to the work of Mahani *et al.* (2015) in which the contact angle decreases with the decreases of zeta potential. In a summary, the main mechanism resulting in the wettability alteration is the surface charge change in this study. However, some further investigation on surface charge change for rock-brine-gas is still necessary.

Second difference of relative permeability curve is the slope of water relative permeability under different conditions. Actually, it is due to a larger viscosity ratio of gas to water in HTHPP, thus there is a higher displacing efficiency and accordingly exhibits a relatively slow decreasing rate under the approximate fluid velocity of all these experiments. This difference is also suggested by more water production before breakthrough under HTHPP (Tab. 3), and subsequently brings a slightly lower water relative permeability at the critical gas saturation.

In addition, we observe a more convex curve of the gas phase for cores c and f under AC, as well as a curve shape change of core e from HTHPP to AC. These shape changes demonstrate a weaker interference between two fluids and a favorable mobility under HTHPP.

4 Conclusion

We performed gas–water two-phase relative permeability under two different conditions using tight gas carbonate samples, especially for the condition of HTHPP (80 °C, 38 MPa) which is scarcely attained in published literature. Our conclusions are as follows:

1. There exist two contrary gas relative permeability curve shapes, corresponding to the different micropore structure among these core samples. The convex relative permeability curve is caused by the strong heterogeneity – discontinuity of pore space, reflecting an insufficient flow in this tight gas carbonate. On the contrary, the concave curve is accompanied by a better pore connectivity. In addition, without considering the fractured core sample, relative permeability under HTHPP shows a general linkage with absolute permeability: characteristic data such as critical gas saturation and residual water saturation decrease with the increase of absolute permeability.
2. Gas relative permeability can be significantly overestimated in conventional low-pressure condition. Based on Klinkenberg theory and a newly developed slip factor model, we calibrated the gas relative permeability obtained at AC and it suggests that the overestimation of gas relative permeability could up to 41.72%–52.34% for three different samples under an assumed core heterogeneity ($m = 1.2$).
3. Comparison of relative permeability between different conditions shows that relative permeability curve switches to a higher gas saturation when the wettability change from strong water-wet to less water-wet, exhibiting a relatively higher water relative permeability and lower gas relative permeability under certain saturation. Wettability alteration in this dolomite reservoir is mainly caused by charge change on mineral surface. In addition, the larger viscosity ratio of gas to water and the weaker fluids interference under HTHPP are respectively responsible for the flatter water relative permeability curve and the less convex gas relative permeability curve.

Acknowledgments. The authors are grateful to the National Natural Science Foundation of China (51774300), the National Science and Technology Major Project of China (2016ZX05015-003) for their financial support.

References

Alotaibi M.B., Nasr-El-Din H.A., Fletcher J.J. (2011) Electrokinetics of limestone and dolomite rock particles, *SPE Reserv. Eval. Eng.* **14**, 5, 594–603.

Alroudhan A., Vinogradov J., Jackson M.D. (2016) Zeta potential of intact natural limestone: Impact of potential-determining ions Ca, Mg and SO_4, *Colloids Surf., A* **493**, 83–98.

Anderson W.G. (1987) Wettability literature survey part 5: The effects of wettability on relative permeability, *J. Pet. Technol.* **39**, 11, 1453–1468.

Austad T., Shariatpanahi S.F., Strand S., Black C.J.J., Webb K.J. (2011) Conditions for a lowsalinity enhanced oil recovery (EOR) effect in carbonate oil reservoirs, *Energy Fuels* **26**, 1, 569–575.

Bachu S., Bennion B. (2008) Effects of in-situ conditions on relative permeability characteristics of CO_2-brine systems, *Environ. Geol.* **54**, 1707–1722.

Bignonnet F., Duan Z., Egermann P., Jeannin L., Skoczylas F. (2016) Experimental measurements and multi-scale modeling

of the relative gas permeability of a caprock, *Oil Gas Sci. Technol. - Rev. IFP Energies nouvelles* **71**, 55.

CMG (2003) *Win WinProp-phase property program*, Computer Modelling Group (CMG) Ltd, Calgary, Canada. User's Guide

Counsil J.R. (1979) Steam-water relative permeability, *PhD Thesis*, Stanford University, Palo Alto, CA.

Cumella S.P., Shanley K.W., Camp W.K. (2014) Li et al. translation, *Understanding, exploring, and developing tight-gas sands*, Petroleum Industry Press, Beijing, China.

Delshad M., Bhuyan D., Pope G.A., Lake L.W. (1986) Effect of capillary number on the residual saturation of a three-phase micellar solution, *Presented at SPE Enhanced Oil Recovery Symposium*, April 20–23, Tulsa, Oklahoma, SPE 14911-MS.

Esmaeilzadeh P., Sadeghi M.T., Bahramian A. (2018) Production improvement in gas condensate reservoirs by wettability alteration, using superamphiphobic titanium oxide nanofluid, *Oil Gas Sci. Technol. - Rev. IFP Energies nouvelles* **73**, 46.

Estes R.K., Fulton P.F. (1956) Gas slippage and permeability measurements, *J. Pet. Technol.* **8**, 69–73.

Fulton P.F. (1951) The effect of gas slippage on relative permeability measurements, *Producers Monthly* **15**, 14–19.

Hiorth A., Cathles L.M., Madland M.V. (2010) The impact of pore water chemistry on carbonate surface charge and oil wettability, *Transp. Porous Med.* **85**, 1, 1–21.

Islam M.R. (2015) Chapter 2 – World gas reserve and the role of unconventional gas, in: *Unconventional Gas Reservoirs*, Gulf Professional Publishing, Boston, MA, pp. 9–69.

Johnson E.F., Bossler D.P., Bossler V.O.N. (1958) Calculation of relative permeability from displacement experiments, *Trans. AIME* **216**, 370–372.

Liu X., Yan J., Liu Y. (2011) Slippage effect and quasi starting pressure in low permeability water-bearing gas reservoirs, *Presented at SPE Reservoir Characterisation and Simulation Conference and Exhibition*, October 9–11, Abu Dhabi, UAE, 145803-MS

Li J., Chen Z., Wu K., Li R., Xu J., Liu Q., Qu S., Li X. (2018) Effect of water saturation on gas slippage in tight rocks, *Fuel* **225**, 519–532.

Li K., Horne R.N. (2001) Gas slippage in two-phase flow and the effect of temperature, *Presented at SPE Western Regional Meeting*, March 26–30, Bakersfield, CA, SPE 68778-MS.

Li S., Dong M., Li Z. (2009) Measurement and revised interpretation of gas flow behavior in tight reservoir cores, *J. Pet. Sci. Eng.* **65**, 81–88.

Mahani H., Keya A.L., Berg S., Bartels W.B., Nasralla R., Rossen W.R. (2015) Insights into the mechanism of wettability alteration by low-salinity flooding (LSF) in carbonates, *Energy Fuels* **29**, 3, 1352–1367.

McCaffery F.G. (1973) The effect of wettability on relative permeability and imbibition in porous media, *PhD Thesis*, University of Calgary, Calgary, Canada.

Moore T.F., Slobod R.L. (1956) The effect of viscosity and capillarity on the displacement of oil by water, *Producers Monthly* **20**, 20–30.

Nasralla RA., Snippe JR., Farajzadeh R. (2015) Coupled geochemical-reservoir model to understand the interaction between low salinity brines and carbonate rock, *Presented at SPE Asia Pacific Enhanced Oil Recovery Conference*, August 11–13, Kuala Lumpur, Malaysia, SPE 174661-MS.

Pini R., Benson S.M. (2013) Simultaneous determination of capillary pressure and relative permeability curves from core-flooding experiments with various fluid pairs, *Water Resour. Res.* **49**, 3516–3530.

Reynolds C.A., Krevor S. (2015) Characterizing flow behavior for gas injection: Relative permeability of CO_2-brine and N_2-water in heterogeneous rocks, *Water Resour. Res.* **51**, 9464–9489.

Rose W.D (1948) Permeability and gas-slippage phenomena, *Presented at 28th Annual Mtg. Topical Committee on Production Technology.*

Rushing J.A., Newsham K.E., Van Fraassen K.C. (2003) Measurement of the two-phase gas slippage phenomenon and its effect on gas relative permeability in tight gas sands, *Presented at SPE Annual Technical Conference and Exhibition*, October 5–8, Denver, Colorado, 84297-MS.

Sampath K., Keighin C.W. (1982) Factors affecting gas slippage in tight sandstones of cretaceous age in the Uinta basin, *J. Pet. Technol.* **34**, 2715–2720.

Sander R., Pan Z., Connell L.D. (2017) Laboratory measurement of low permeability unconventional gas reservoir rocks: A review of experimental methods, *J. Nat. Gas Sci. Eng.* **37**, 248–279.

Satter A., Iqbal G.M. (2016) 22 – Unconventional gas reservoirs, in: *Reservoir Engineering*, Gulf Professional Publishing, Boston, MA, pp. 389–425.

Wei X., Chen J., Zhang D., Yan X., Ren J., Yan T. (2017) Geological characteristics and reservoir forming conditions of large area tight carbonate gas in eastern Ordos Basin, China, *Nat. Gas Geosci.* **28**, 677–686.

Yousef A.A., Al-Saleh S.H., Al-Kaabi A., Al-Jawfi M.S. (2011) Laboratory investigation of the impact of injection-water salinity and ionic content on oil recovery from carbonate reservoirs, *SPE Reserv. Eval. Eng.* **14**, 5, 578–593.